Absorption spectra of tri-*s*-triazines: time dependent density functional theory calculations

Wenxu Zheng,[a] Ning-Bew Wong,*[a] Wai-Kee Li[b] and Anmin Tian*[c]

Received (in St Louis, MO, USA) 17th November 2005, Accepted 30th June 2006
First published as an Advance Article on the web 27th July 2006
DOI: 10.1039/b516353f

The singlet and triplet vertical excited states of tri-*s*-triazines have been investigated by using time-dependent density functional theory (TDDFT). The solvation effects on the excitation energies for tri-*s*-triazines in ethanol are taken into account by using the polarized continuum model (PCM). The computed results show a good agreement with the available UV/Vis absorption spectra.

1. Introduction

Over a decade ago, some theoreticians predicted that the hardness of several structures of carbon nitride (C_3N_4) could exceed that of diamond.[1,2] This motivated numerous synthetic efforts.[3–8] The *s*-triazines (including melamine, $C_3N_3(NH_2)_3$) are often used as synthetic precursors for the carbon nitride materials. However, as pointed out by Kroke *et al.*,[9] tri-*s*-triazines are more suitable as a starting fragment for the synthesis of extended C_3N_4 solids, because they provide a bigger building block, which is composed of three *s*-triazine units. This suggestion has drawn much attention to the tri-*s*-triazine-based molecules. The study of tri-*s*-triazines can be traced back to the 1830s.[10,11] Owing to their insolubility and chemical inertness, the tri-*s*-triazines remained structural puzzles for more than a century. It was not until 1937 that Pauling and Sturdivant carried out crystallography experiments and showed that the nucleus of tri-*s*-triazines has a planar structure consisting of three fused *s*-triazine rings.[12] Pauling apparently maintained a very long interest in tri-*s*-triazines and, for reasons unknown, the molecular formula of 2-azido-5,8-dihydroxy-tri-*s*-triazine was preserved on his office chalkboard at the time of his death in 1994.[13] However, in the past decades, only the tri-*s*-triazine molecule itself was studied in detail.[14–16] Its structural and spectroscopic properties including X-ray crystal structure analysis were studied. In addition, its UV photoelectron spectra were taken and *ab initio* calculations were performed in order to explain its low basicity and high stability.[14–16] In 2002, Kroke *et al*. synthesized 2,5,8-trichloro-tri-*s*-triazine and found that it is a promising starting material for numerous compounds including graphitic C_3N_4 phases.[9] In 2003, Schnick and coworkers determined the crystal structure of 2,5,8-triamino-tri-*s*-triazine,[17] and in 2004, Gillan *et al*. reported the synthesis and crystal structure of 2,5,8-triazido-tri-*s*-triazine.[18] To the best of our knowledge, other tri-*s*-triazines were only briefly mentioned and no structural characterization on them was reported.[19]

Previously, we investigated the geometric and electronic structures, HEDM (high energy density material) properties, isomerism, molecular interactions and hyper polarizabilities of the tri-*s*-triazine-based molecules in details using *ab initio* methods.[20–23] In this work, the absorption spectra of tri-*s*-triazines are characterized with time dependent density functional theory (TDDFT).

The method of TDDFT has been developed and formulated for the calculation of excitation energies within the DFT framework.[24–27] Properties of the excited states can be determined with DFT from the molecule's linear response to an external continuous wave field. A large data pool has been accumulated over the past years to promote TDDFT as a powerful tool for the calculation of vertical electronic excitation spectra, particularly for valence-like transitions.[28–31] It has been claimed that reliable vertical excitation energies to Rydberg states can only be computed using more sophisticated tools, such as the asymptotically corrected potentials.[32,33] Barone *et al*. have found that the PBE0 model,[34] a hybrid Hartree–Fock (HF)/Kohn–Sham (KS) approach based on the Perdew–Burke–Erzenrhof (PBE) exchange–correlation functional,[35] could provide vertical excitation energies in good agreement with experimental data.[36,37] Furthermore, this method could yield excitations to both valence and low-lying Rydberg states with similar accuracy, even in the presence of non-negligible contributions from double excitations.[37] Excited states can also be modeled in the presence of a solvent[38,39] using the TDDFT method. In the present work, to compute solvent shifts of UV spectra, we apply a recent reformulation of the polarizable continuum model (PCM) to TDDFT.

2. Computational details

All calculations were performed using the Gaussian 03 package.[40]

In TDDFT calculations, the B3LYP and PBE0 functionals combined with aug-cc-pVDZ basis set are chosen, due to their versatile usability. In particular, B3LYP is a standard for geometry optimizations, and the PBE0 parameter-free hybrid

[a] *Department of Biology and Chemistry, City University of Hong Kong, Kowloon, Hong Kong. E-mail: bhnbwong@cityu.edu.hk*
[b] *Department of Chemistry, The Chinese University of Hong Kong, Shatin, Hong Kong*
[c] *Faculty of Chemistry, Sichuan University, Chengdu, Sichuan, 610064, P. R. China. E-mail: suqcp@mail.sc.cninfo.net*

model is based on the previous works of Becke[41] and Perdew,[42] which yield reliable results for several physico-chemical properties including excitation energies and low-lying Rydberg transitions.

The ground state geometries of all molecules were obtained from optimizations using the B3LYP functional[43,44] with the aug-cc-pVDZ (5d) basis set.[45] The results obtained by this method are similar to those yielded by using PBE0 functional. Since the ground state geometries are employed for all excited state calculations, the theoretical excitation energies correspond to the vertical transitions and they can be identified as band maxima in the experimental spectra.

It is well known that solvent has a great influence on the electronic spectra owing to the interaction between the solute and the solvents. In this work, the non-equilibrium solvent effect in vertical transition processes was described using the PCM model[39,46,47] to all calculations. The reliability of this model for both ground and excited states is well documented. In this formulation,[48,49] the solvated system is partitioned into a target molecule (the solute) and the surrounding solvent, which is modeled as a continuum, infinite, homogeneous, and generally isotropic medium, characterized by its dielectric properties. The solute is assumed to be inside a molecular-shaped cavity, and the electrostatic solute–solvent interactions are calculated by introducing an apparent charge distribution spread on the cavity surface. So the explicit interactions between solute and solvent molecules, such as hydrogen bonding and dispersion force, cannot be evaluated. The current PCM version is called implicit volume charge (IVC)-PCM, in which the contribution of the electronic charge lying outside the solute cavity is taken into account more effectively than in the previous PCM versions. At the same time, the error connected with the numerical integration of the Poisson equation is reduced.

The simulated spectra were obtained by broadening the theoretical line spectra with Gaussian functions, *i.e.*,

$$I(\tilde{\nu}) = \sum_i f_i \exp\left[-\frac{1}{2}\left(\frac{\tilde{\nu}-\tilde{\nu}_i}{\sigma}\right)^2\right]$$

where σ, equal to 1300 cm^{-1}, is the Gaussian centered width at the peak number i with wavenumber $\tilde{\nu}_i$ and oscillator strength f_i. This procedure roughly accounts for the finite experimental resolution, vibrational and rotational broadening, finite lifetime, and nonvertical transition effects.

3. Results and discussion

The ground-state geometries of the tri-*s*-triazines studied in this work were optimized using the B3LYP functional with the aug-cc-pVDZ basis set both in gas phase and in solution (using the PCM method). Comparison of the gas phase and solution results shows very little difference. These geometries were reported in detail in our previous work.[20] The molecular structures of the tri-*s*-triazines, along with the geometrical parameters, are illustrated in Fig. 1. As shown in the figure, all the optimized tri-*s*-triazine-based molecules have D_{3h} symmetry, except that triazido-tri-*s*-triazine belongs to the C_{3h} point group. The tri-*s*-triazine ring in all species maintains a rigid plane geometry, and the C–N bonds on the periphery of the ring have a uniform bond length ranging from 1.310 to 1.347 Å, which lie between a normal C–N single bond length (1.470 Å) and a normal C═N double bond length (1.280 Å).

3.1. Gas-phase absorption

The computed vertical excitation energies in the gas-phase and the oscillator strengths of *s*-triazine and tri-*s*-triazines are listed in Tables 1–7. Starting from the spin-allowed singlet → singlet transitions, thirty singlet-excited states have been calculated at the optimized structure of the ground state for each species. The transitions from the ground state to several singlet excited states have zero oscillator strength and hence they do not contribute to the absorption spectra. In the tables, only those transitions with oscillator strengths above 0.01 are listed, together with the available experimental data. The results are also presented graphically in Fig. 2. The UV/Vis spectrum obtained from PBE0 calculation is shown in the top panel of each figure. Although all the excitation energies calculated using PBE0 are slightly higher than those calculated using B3LYP, they have similar orders of magnitude. From these tables, we can find that the B3LYP and PBE0 functionals give almost the same transition order with a few exceptions occurring at the high-energy end of the spectra of *s*-triazine, trifluoride-tri-*s*-triazine and triamino-tri-*s*-triazine. That is to say, the results obtained with two methods are similar, and from now on we will confine our discussion to the B3LYP results. The calculated UV/Vis spectrum of *s*-triazine in the gas phase has an absorption maximum at 7.75 eV, which is in excellent agreement with experiment[50] (7.76 eV). Even a weak band in the low-energy region (4.53 eV) is also in excellent agreement with experiment (4.59 eV). Below 4 eV, no excited state or absorption feature could be found. For tri-*s*-triazine, there are two strong bands at around 4.48 and 6.03 eV, while the corresponding experimental data are 4.07 and 5.66 eV, respectively, with a difference[15] of about 0.4 eV for each band. The strongest absorption band of the tri-*s*-triazine exhibits red shift with respect to that of the *s*-triazine. In the UV/Vis spectra of trisubstituted tri-*s*-triazines shown in Fig. 2, we see a strong band at 7.18 eV and two weak bands at 4.80 and 6.09 eV for trifluoride-tri-*s*-triazine, a strong band at 6.01 eV and a weak band at 5.23 eV for triamino-tri-*s*-triazine, a strong band at 4.60 eV for trinitro-tri-*s*-triazine and two strong bands at 4.30 and 5.20 eV for triethynyl-tri-*s*-triazine, and two strong bands at 4.53 and 5.27 eV for triazido-tri-*s*-triazine. Except triethynyl-tri-*s*-triazine, all the strongest bands are blue-shifted with respect to that of tri-*s*-triazine, and their oscillator strengths are higher than that of the tri-*s*-triazine.

Common model of an excited state in the one-electron picture describes an electron relocated from an occupied MO to a virtual MO. However, the excited states in this work are shown to be best described in terms of multiconfigurations that a given optical transition comprises a linear combination of several occupied-to-virtual MO excitations. Assignment of the character of each excited state is based on the compositions of the occupied and virtual MOs of the dominant configuration(s) for that excited state. As an example, we have selected the excited states with the highest oscillator strengths in tri-*s*-

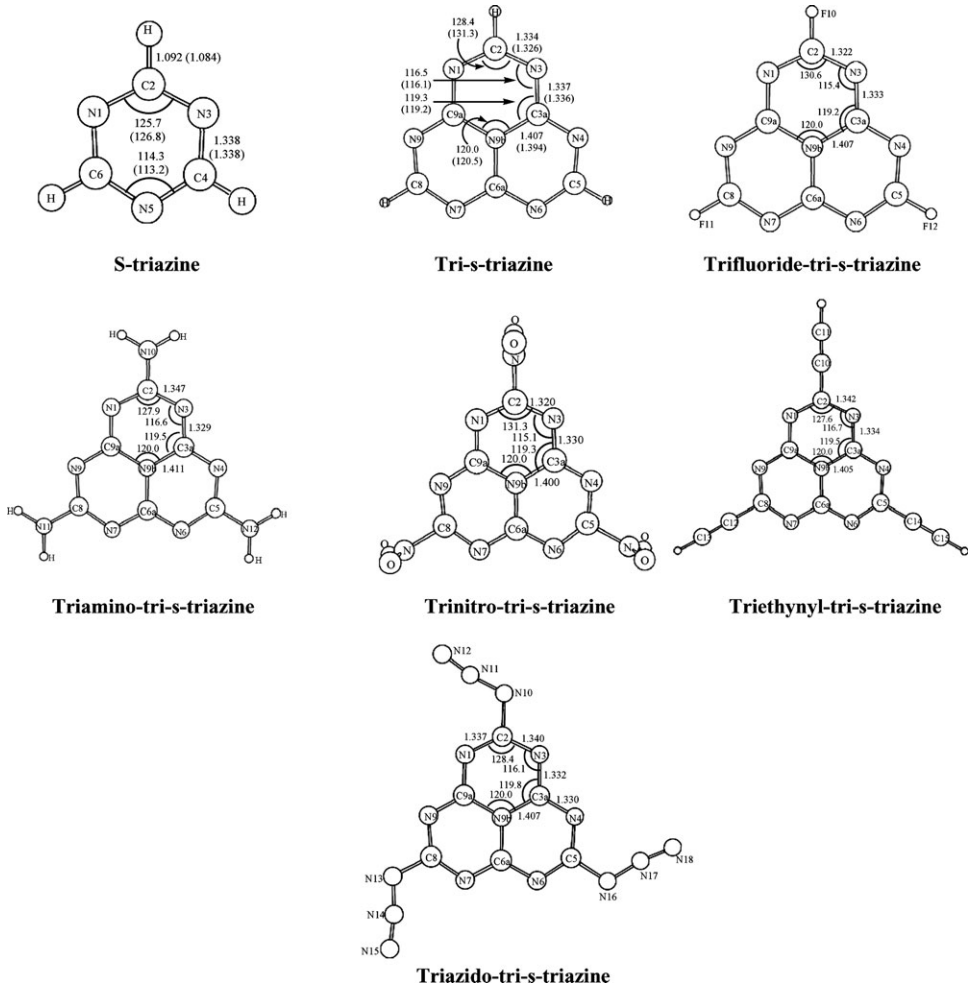

Fig. 1 Optimized molecular structures for *s*-triazine and tri-*s*-triazines, with bond lengths in Å and bond angles in °. Experimental data for *s*-triazine and tri-*s*-triazine are given in parentheses.

triazines for analysis. Contour maps of the corresponding MOs are illustrated in Fig. 3. For the excited state S_{17} of tri-*s*-triazine, the dominant excitation is 36 → 45. Since the occupied orbital (36) is a π-type orbital and the virtual orbital (45) is a π*-type orbital, the transition is denoted as a π → π* transition. For the excited state S_{28} in trifluoride-tri-*s*-triazine, the dominant excitation is 50 → 58. The occupied orbital (50) is an n-type orbital mainly located on the fluorine atom, and the virtual orbital (58) is a π*-type orbital around the tri-*s*-triazine ring. Hence, the transition is denoted as an n → π* excitation. For the excited state S_{23} in triamino-tri-*s*-triazine, the dominant excitation is 50 → 59, and the occupied orbital (50) is an n-type orbital located on the amino nitrogen atom and the virtual orbital (59) is a π*-type orbital. Thus the transition is denoted as an n → π* excitation. For the excited state S_{17} in trinitro-tri-*s*-triazine, the dominant excitation is 77 → 79. The occupied orbital (77) is an n-type orbital, and the virtual orbital (79) is a π*-type orbital. Hence the transition is denoted as an n → π* excitation. For the excited state S_{10} in triethynyl-tri-*s*-triazine, the dominant excitation is 58 → 63. The occupied orbital (58) is a π-type orbital located on the C≡C bond of the ethynyl and the virtual orbital (63) is a π*-type orbital. Thus the transition is denoted as a π → π* excitation. For the excited state S_7 in triazido-tri-*s*-triazine, the dominant excitation is 72 → 75. The occupied orbital (72) is an n-type orbital, and the virtual orbital (75) is a π*-type orbital. So the transition is denoted as an n → π* excitation. From the above discussion, we may conclude that only the excited states with the highest oscillator strengths in tri-*s*-triazine and triethynyl-tri-*s*-triazine give π → π* excitations, which lead to relatively larger transition energies.

The 30 lowest-energy triplet excited states for *s*-triazine and tri-*s*-triazines were also calculated using analogous TDDFT methodology. Only the first five triplet excited states are listed in Tables 1–7. Most of them are mixed with the singlets. As predicted by Hund's rule, transitions to the triplet states require lower energy than those to the singlets. For example, in tri-*s*-triazine, the first triplet vertical transition calculated by B3LYP takes place at 2.65 eV, which is 0.21 eV lower than that of the first singlet excited state (2.86 eV). Both of these transitions are represented by 44 → 45. The TDDFT results do not provide information on singlet–triplet absorption intensities since spin–orbit coupling effects are not included in current TDDFT approaches. So the oscillator strengths in

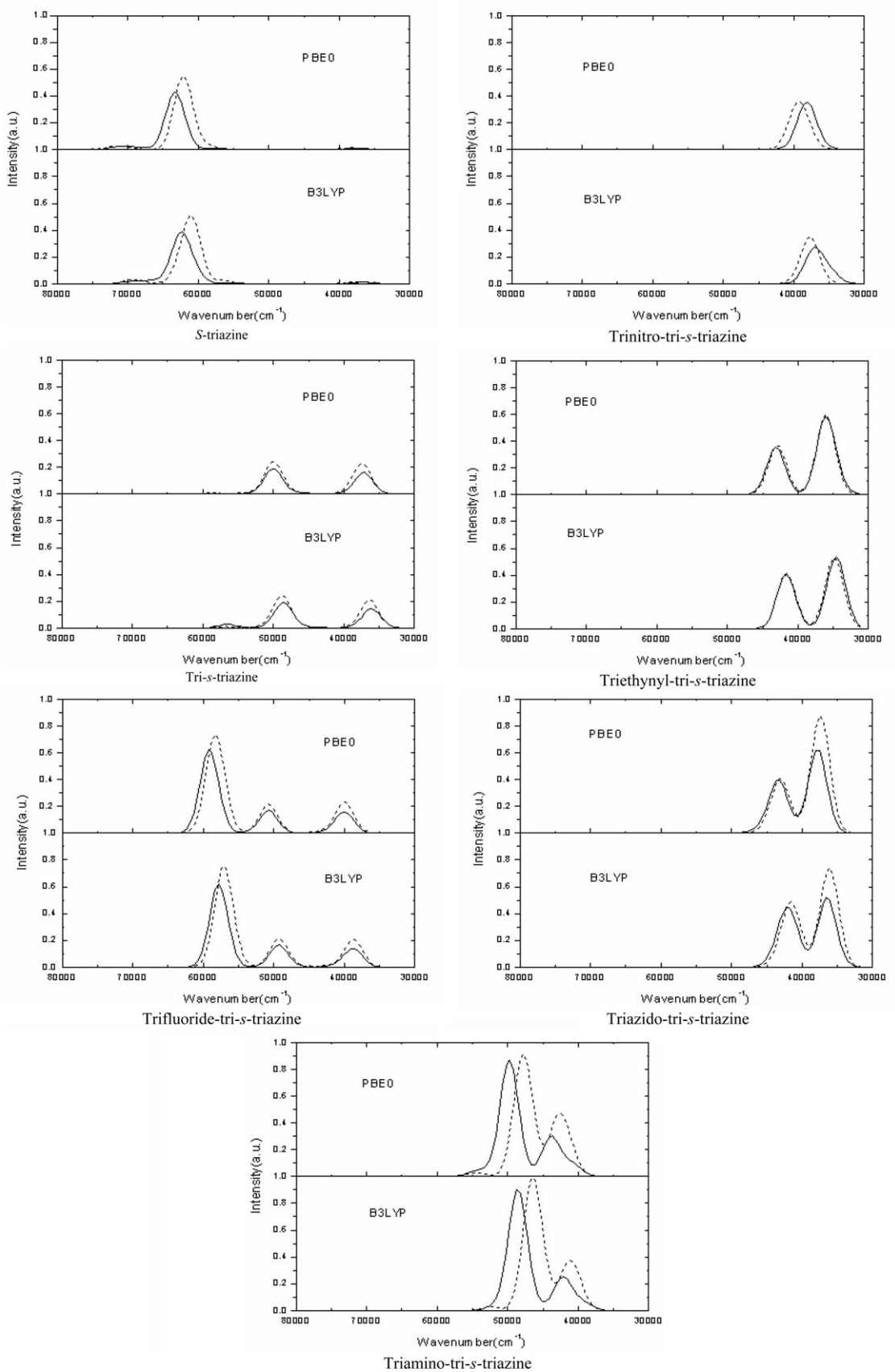

Fig. 2 Calculated absorption spectra in the gas phase (solid curves) and in ethanol (dotted curves) for *s*-triazine and tri-*s*-triazines.

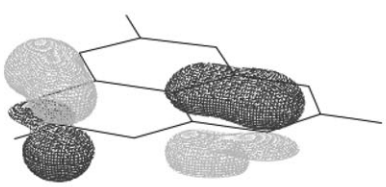

Tri-*s*-triazine MO (36, O)

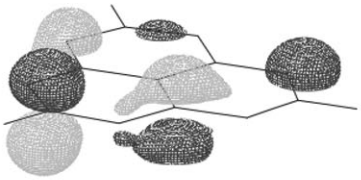

Tri-*s*-triazine MO (45, V)

Trifluoride-tri-*s*-triazine MO (50, O)

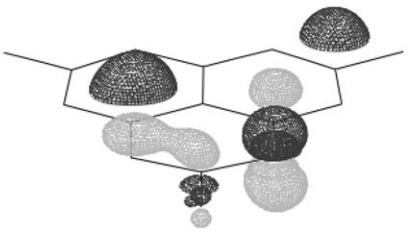

Trifluoride-tri-*s*-triazine MO (58, V)

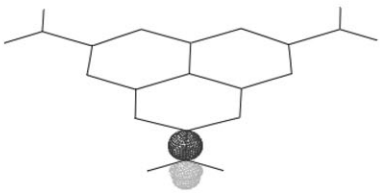

Triamino-tri-*s*-triazine MO (50, O)

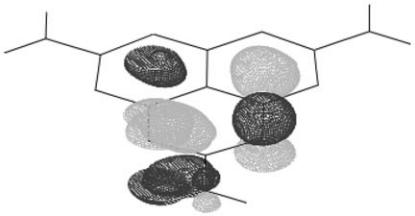

Triamino-tri-*s*-triazine MO (59, V)

Trinitro-tri-*s*-triazine MO (77, O)

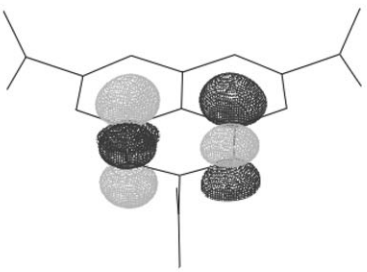

Trinitro-tri-*s*-triazine MO (79, V)

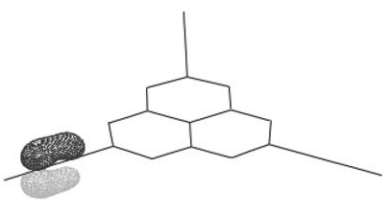

Triethynyl-tri-*s*-triazine MO (58, O)

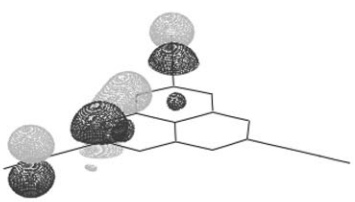

Triethynyl-tri-*s*-triazine MO (63, V)

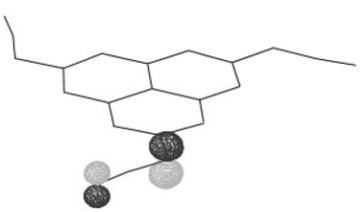

Triazido-tri-*s*-triazine MO (72, O)

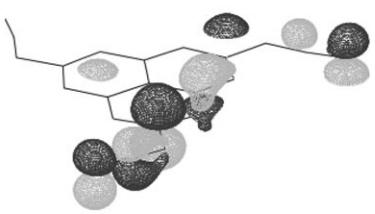

Triazido-tri-*s*-triazine MO (75, V)

Fig. 3 Dominant occupied (O) and virtual (V) orbitals for excited states with highest oscillator strength of tri-*s*-triazines.

Table 1 Selected calculated excitation energies (E), wavelengths (λ), oscillator strengths (f), and dominant excitation character for singlet (S_n) and triplet (T_n) states of the *s*-triazine in the gas phase and comparison with experimental data

B3LYP					PBE0					
Excited state	Main configuration	E/eV	λ/nm	f	Excited state	Main configuration	E/eV	λ/nm	f	Exp E/eV
Singlet excited state										
S_4 (A_2'')	0.49(20 → 22) − 0.49(21 → 23)	4.53	273	0.012	S_2 (A_2'')	− 0.48(20 → 23) + 0.48(21 → 22)	4.62	268	0.013	4.59
S_6 (E′)	0.70(21 → 24)	6.86	181	0.009	S_7 (E′)	0.70(21 → 24)	7.14	174	0.010	
S_7 (E′)	0.70(20 → 24)	6.86	181	0.009	S_8 (E′)	0.70(20 → 24)	7.14	174	0.010	
S_{12} (E′)	0.49(20 → 25) + 0.49(21 → 26)	7.50	165	0.076	S_{12} (E′)	−0.24(18 → 23) + 0.24(19 → 22) + 0.41(20 → 25) − 0.41(21 → 26)	7.78	159	0.252	
S_{13} (E′)	−0.49(20 → 26) + 0.49(21 → 25)	7.50	165	0.076	S_{13} (E′)	0.24(18 → 23) + 0.24(19 → 22) + 0.41(20 → 25) + 0.41(21 → 26)	7.78	159	0.252	
S_{15} (E′)	0.41(18 → 23) + 0.41(19 → 22)	7.75	160	0.361	S_{15} (E′)	0.35(18 → 22) + 0.35(19 → 23) − 0.28(20 → 26) − 0.28(21 → 25)	7.89	157	0.198	7.76
S_{16} (E′)	−0.41(18 → 22) + 0.41(19 → 23)	7.75	160	0.361	S_{16} (E′)	0.34(18 → 23) − 0.34(19 → 22) + 0.28(20 → 25) − 0.28(21 → 26)	7.89	157	0.198	
S_{19} (E′)	0.70(21 → 28)	8.21	151	0.025	S_{19} (E′)	0.70(21 → 28)	8.49	146	0.018	
S_{20} (E′)	0.70(20 → 28)	8.21	151	0.025	S_{20} (E′)	0.70(20 → 28)	8.49	146	0.018	
S_{23} (E′)	0.49(20 → 29) + 0.49(21 → 30)	8.57	145	0.013	S_{23}(A_1'')	0.49(15 → 22) + 0.49(16 → 23)	8.81	141	0.006	
S_{24} (E′)	−0.49(20 → 30) + 0.49(21 → 29)	8.57	145	0.013	S_{24} (E′)	0.49(20 → 30) + 0.49(21 → 29)	8.83	140	0.016	
S_{27}(A_1'')	0.49(15 → 22) + 0.49(16 → 23)	8.71	142	0.006	S_{25} (E′)	0.49(20 → 29) − 0.49(21 → 30)	8.83	140	0.016	
Triplet excited state										
T_1(A_2'')	−0.52(20 → 22) + 0.52(21 → 23)	3.89	319	0.000	T_1 (A_2'')	−0.10(17 → 37) + 0.52(20 → 23) –0.52(21 → 22)	3.91	317	0.000	
T_2 (E″)	0.51(20 → 22) + 0.51(21 → 23)	4.09	303	0.000	T_2 (E″)	0.51(20 → 23) + 0.11(20 → 37) + 0.51(21 → 22)	4.13	300	0.000	
T_3 (E″)	0.51(20 → 23) − 0.51(21 → 22)	4.09	303	0.000	T_3 (E″)	0.51(20 → 22) − 0.51(21 → 23) + 0.11(21 → 37)	4.13	300	0.000	
T_4(A_1'')	0.51(20 → 23) + 0.51(21 → 22)	4.31	288	0.000	T_4 (A_2')	0.18(14 → 37) − 0.60(18 → 22) + 0.60(19 → 23)	4.22	294	0.000	
T_5 (A_2')	0.16(14 → 35) − 0.59(18 → 23) + 0.59(19 → 22)	4.38	283	0.000	T_5 (A_1'')	0.51(20 → 22) + 0.51(21 → 23)	4.38	283	0.000	

Table 2 Selected calculated excitation energies (E), wavelengths (λ), oscillator strengths (f), and dominant excitation character for singlet (S_n) and triplet (T_n) states of the tri-*s*-triazine in the gas phase and comparison with experimental data

B3LYP					PBE0					
Excited state	Main configuration	E/eV	λ/nm	f	Excited state	Main configuration	E/eV	λ/nm	f	Exp E/eV
Singlet excited state										
S_5 (E′)	0.15(36 → 45) + 0.64(44 → 47)	4.48	277	0.143	S_5 (E′)	−0.13(37 → 45) + 0.65(44 → 46)	4.61	269	0.159	4.07
S_6 (E′)	−0.15(37 → 45) + 0.64(44 → 46)	4.48	277	0.143	S_6 (E′)	0.13(36 → 45) + 0.65(44 → 47)	4.61	269	0.159	
S_9 (A_1'')	0.15(38 → 45) + 0.48(41 → 47) + 0.48(42 → 46)	4.68	265	0.004	S_7 (A_1'')	0.16(38 → 45) + 0.48(41 → 47) + 0.48(42 → 46)	4.81	258	0.004	4.16
S_{15} (A_2'')	0.66(38 → 45) − 0.11(39 → 47) + 0.11(40 → 46) − 0.10(41 → 47) − 0.10(42 → 46)	5.46	227	0.006	S_{15}(A_2'')	0.65(38 → 45) − 0.14(39 → 47) + 0.14(40 → 46) − 0.11(41 → 47) − 0.11(42 → 46)	5.70	217	0.008	
S_{17} (E′)	−0.23(35 → 46) + 0.64(36 → 45)	6.03	206	0.188	S_{16} (E′)	−0.23(35 → 46) + 0.64(36 → 45)	6.20	200	0.188	5.66
S_{18} (E′)	−0.23(35 → 47) + 0.64(37 → 45)	6.03	206	0.188	S_{17} (E′)	−0.23(35 → 47) + 0.64(37 → 45)	6.20	200	0.187	
S_{22}(A_2'')	−0.16(38 → 45) − 0.48(39 → 47) + 0.48(40 → 46)	6.32	196	0.005	S_{22}(A_2'')	0.20(38 → 45) − 0.47(39 → 47) − 0.47(40 → 46)	6.61	188	0.005	
S_{29} (E′)	0.18(35 → 46) + 0.35(36 → 47) + 0.35(37 → 46) + 0.45(44 → 53)	6.99	177	0.004	S_{28} (E′)	0.20(35 → 46) + 0.36(36 → 47) − 0.36(37 → 46) + 0.42(44 → 53)	7.25	171	0.005	
S_{30} (E′)	0.68(42 → 48)	7.00	177	0.023	S_{29} (E′)	0.20(35 → 47) + 0.36(36 → 46) –0.36(37 → 47) + 0.42(44 → 54)	7.25	171	0.005	
Triplet excited state										
T_1 (A_2')	0.72(44 → 45)	2.65	468	0.000	T_1 (A_2')	0.73(44 → 45)	2.72	156	0.000	
T_2 (E′)	0.76(44 → 46)	3.30	376	0.000	T_2 (E′)	0.77(44 → 47)	3.34	371	0.000	
T_3 (E′)	0.76(44 → 47)	3.30	376	0.000	T_3 (E′)	0.76(44 → 46)	3.34	371	0.000	
T_4 (A_1'')	−0.13(41 → 46) + 0.13(42 → 47) + 0.69(43 → 45)	3.57	348	0.000	T_4 (A_1'')	−0.16(41 → 46) + 0.16(42 → 47) + 0.67(43 → 45)	3.70	335	0.000	
T_5 (E″)	0.69(42 → 45) + 0.15(43 → 47)	3.61	343	0.000	T_5 (E″)	0.68(41 → 45) − 0.18(43 → 46)	3.72	333	0.000	

Table 3 Selected calculated excitation energies (E), wavelengths (λ), oscillator strengths (f), and dominant excitation character for singlet (S_n) and triplet (T_n) states of the trifluoride-tri-*s*-triazine in the Gas phase

B3LYP					PBE0				
Excited state	Main configuration	E/eV	λ/nm	f	Excited state	Main configuration	E/eV	λ nm	f
Singlet excited state									
S_5 (E′)	0.14(51 → 57) + 0.65(56 → 58)	4.80	258	0.137	S_5 (E′)	−0.12(52 → 57) + 0.65(56 → 58)	4.95	250	0.156
S_6 (E′)	−0.14(52 → 57) + 0.65(56 → 59)	4.80	258	0.137	S_6 (E′)	0.12(51 → 57) + 0.65(56 → 59)	4.95	250	0.156
S_9(A_1'')	0.49(53 → 59) + 0.49(54 → 58)	5.07	244	0.009	S_7 (A_1'')	0.49(53 → 59) + 0.49(54 → 58)	5.21	238	0.009
S_{13} (E′)	−0.26(50 → 58) + 0.63(52 → 57)	6.09	203	0.163	S_{13} (E′)	−0.25(50 → 59) + 0.64(52 → 57)	6.29	197	0.168
S_{14} (E′)	−0.26(50 → 59) + 0.63(51 → 57)	6.09	203	0.163	S_{14} (E′)	−0.25(50 → 58) + 0.64(51 → 57)	6.29	197	0.168
S_{19}(A2″)	0.65(47 → 57) + 0.18(48 → 58) − 0.18(49 → 59)	6.53	190	0.003	S_{20}(A_2'')	0.63(47 → 57) + 0.20(48 → 59) − 0.20(49 → 58)	6.79	183	0.004
S_{22} (E′)	0.11(44 → 57) + 0.38(50 → 58) + 0.36(51 → 59) − 0.36(52 → 58) − 0.23(56 → 64)	6.93	179	0.002	S_{22} (E′)	0.11(44 → 57) + 0.43(50 → 58) + 0.12(51 → 57) + 0.34(51 → 59) + 0.34(52 → 58) + 0.20(56 → 65)	7.16	173	0.023
S_{23} (E′)	0.11(45 → 57) + 0.38(50 → 59) + 0.36(51 → 58) + 0.36(52 → 59) + 0.23(56 → 65)	6.93	179	0.002	S_{23} (E′)	0.11(45 → 57) + 0.43(50 → 59) + 0.34(51 → 58) + 0.12(52 → 57) − 0.34(52 → 59) + 0.20(56 → 64)	7.16	173	0.023
S_{27}(A_2'')	0.25(47 → 57) − 0.47(48 → 58) + 0.47(49 → 59)	7.18	173	0.001	S_{27} (E′)	0.44(50 → 58) + 0.16(51 → 57) −0.32(51 → 59) − 0.32(52 → 58)	7.35	169	0.611
S_{28} (E′)	0.47(50 → 58) − 0.28(51 → 59) + 0.18(52 → 57) + 0.28(52 → 58)	7.18	173	0.618	S_{28} (E′)	0.44(50 → 59) − 0.32(51 → 58) + 0.16(52 → 57) + 0.32(52 → 59)	7.35	169	0.611
S_{29} (E′)	0.47(50 → 59) + 0.18(51 → 57) − 0.28(51 → 58) − 0.28(52 → 59)	7.18	173	0.618	S_{29}(A_2'')	−0.29(47 → 57) + 0.45(48 → 59) − 0.45(49 → 58)	7.53	165	0.001
Triplet excited state									
T_1(A_2')	0.72(56 → 57)	3.25	381	0.000	T_1 (A_2')	0.72(56 → 57)	3.35	371	0.000
T_2 (E′)	0.75(56 → 59)	3.66	339	0.000	T_2 (E′)	0.75(56 → 59)	3.72	334	0.000
T_3 (E′)	0.75(56 → 58)	3.66	339	0.000	T_3 (E′)	0.75(56 → 58)	3.72	334	0.000
T_4(A_1'')	0.14(53 → 58) − 0.14(54 → 59) + 0.68(55 → 57)	4.21	295	0.000	T_4 (A_1'')	−0.16(53 → 58) + 0.16(54 → 59) + 0.67(55 → 57)	4.36	284	0.000
T_5 (E″)	0.68(53 → 57) + 0.17(55 → 58)	4.25	292	0.000	T_5 (E″)	0.67(53 → 57) − 0.11(53 → 59) + 0.11(54 → 58) − 0.19(55 → 58)	4.38	283	0.000

Table 4 Selected calculated excitation energies (E), wavelengths (λ), oscillator strengths (f), and dominant excitation character for singlet (S_n) and triplet (T_n) states of the triamino-tri-*s*-triazine in the gas phase

B3LYP					PBE0				
Excited state	Main configuration	E/eV	λ/nm	f	Excited state	Main configuration	E/eV	λ/nm	f
Singlet excited state									
S_5 (E′)	−0.18(55 → 57) + 0.64(56 → 58)	4.89	254	0.058	S_5 (E′)	−0.13(54 → 57) + 0.65(56 → 59)	5.06	245	0.088
S_6 (E′)	−0.18(54 → 57) + 0.64(56 → 59)	4.89	254	0.058	S_6 (E′)	−0.13(55 → 57) + 0.65(56 → 58)	5.06	245	0.088
S_7 (E′)	−0.18(50 → 59) − 0.13(54 → 58) + 0.63(55 → 57) − 0.13(55 → 59)	5.23	237	0.235	S_9 (A_2'')	0.49(51 → 59) − 0.49(52 → 58)	5.41	229	0.008
S_8 (E′)	0.18(50 → 58) + 0.63(54 → 57) + 0.13(54 → 59) − 0.13(55 → 58)	5.23	237	0.235	S_{10} (E′)	−0.17(50 → 59) + 0.65(55 → 57)	5.44	228	0.289
S_{11} (A_1'')	0.49(51 → 58) + 0.49(52 → 59)	5.28	235	0.008	S_{11} (E′)	0.17(50 → 58) + 0.65(54 → 57)	5.44	228	0.289
S_{20} (E′)	0.44(50 → 59) − 0.37(54 → 58) − 0.37(55 → 59)	5.69	218	0.020	S_{18} (E′)	0.44(50 → 59) − 0.37(54 → 58) − 0.37(55 → 59)	5.89	210	0.008
S_{21} (E′)	0.44(50 → 58) − 0.37(54 → 59) + 0.37(55 → 58)	5.69	218	0.020	S_{19} (E′)	0.44(50 → 58) − 0.37(54 → 59) + 0.37(55 → 58)	5.89	210	0.008
S_{23} (E′)	0.49(50 → 59) + 0.26(54 → 58) + 0.17(55 → 57) + 0.26(55 → 59) + 0.13(56 → 58)	6.01	206	0.894	S_{23} (E′)	0.49(50 → 58) − 0.14(54 → 57) + 0.28(54 → 59) − 0.28(55 → 58) − 0.12(56 → 59)	6.16	201	0.863
S_{24} (E′)	0.49(50 → 58) − 0.17(54 → 57) + 0.26(54 → 59) − 0.26(55 → 58) − 0.13(56 → 59)	6.01	206	0.894	S_{24} (E′)	0.49(50 → 59) + 0.27(54 → 58) + 0.14(55 → 57) + 0.28(55 → 59) + 0.12(56 → 58)	6.16	201	0.863
S_{28} (A_1')	−0.29(50 → 60) + 0.45(54 → 61) + 0.45(55 → 62)	6.19	200	0.019	S_{27} (A_2'')	−0.31(50 → 60) − 0.43(54 → 62) + 0.43(55 → 61)	6.46	192	0.029
S_{30} (E′)	0.55(51 → 60) − 0.18(51 → 62) + 0.18(52 → 61) − 0.35(53 → 62)	6.40	194	0.036	S_{30} (E′)	0.18(51 → 62) + 0.55(52 → 60) − 0.18(52 → 61) − 0.10(52 → 63) + 0.32(53 → 61)	6.72	184	0.039
Triplet excited state									
T_1 (A_2')	0.71(56 → 57)	3.75	331	0.000	T_1 (A_2')	0.71(56 → 57)	3.85	322	0.000
T_2 (E′)	0.10(54 → 58) + 0.12(55 → 57) + 0.10(55 → 59) + 0.72(56 → 58)	3.89	319	0.000	T_2 (E′)	0.12(54 → 58) + 0.14(55 → 57) + 0.12(55 → 59) + 0.72(56 → 58)	3.95	314	0.000
T_3 (E′)	0.12(54 → 57) − 0.10(54 → 59) + 0.10(55 → 58) + 0.72(56 → 59)	3.89	319	0.000	T_3 (E′)	0.14(54 → 57) − 0.12(54 → 59) + 0.12(55 → 58) + 0.72(56 → 59)	3.95	314	0.000
T_4 (E′)	0.17(50 → 59) + 0.15(54 → 58) + 0.66(55 → 57) + 0.15(55 → 59) − 0.14(56 → 58)	4.45	278	0.000	T_4 (E′)	0.61(50 → 57) − 0.30(54 → 58) + 0.30(55 → 59)	4.56	272	0.000
T_5 (E′)	−0.17(50 → 58) + 0.66(54 → 57) −0.15(54 → 59) + 0.15(55 → 58) −0.14(56 → 59)	4.45	278	0.000	T_5 (E′)	0.19(50 → 59) + 0.16(54 → 58) + 0.65(55 → 57) + 0.16(55 → 59) − 0.16(56 → 58)	4.56	272	0.000

Table 5 Selected calculated excitation energies (E), wavelengths (λ), oscillator strengths (f), and dominant excitation character for singlet (S_n) and triplet (T_n) states of the trinitro-tri-*s*-triazine in the gas phase

B3LYP					PBE0				
Excited state Singlet excited state	Main configuration	E/eV	λ/nm	f	Excited state	Main configuration	E/eV	λ/nm	f
S_6 (E′)	0.68(73 → 78) + 0.15(77 → 80)	4.31	287	0.08	S_{10} (E′)	−0.12(66 → 82) − 0.16(66 → 83) + 0.37(71 → 81) + 0.26(75 → 82) + 0.35(75 → 83) + 0.26(76 → 81)	4.47	277	0.001
S_7 (E′)	0.68(74 → 78) + 0.15(77 → 79)	4.31	287	0.08	S_{11} (E′)	0.16(65 → 83) − 0.12(66 → 81) + 0.37(71 → 82) + 0.26(75 → 81) − 0.26(76 → 82) + 0.35(76 → 83)	4.47	277	0.001
S_{14} (E′)	+ 0.15(66 → 83) − 0.13(69 → 78) + 0.37(71 → 82) − 0.26(75 → 82) + 0.36(75 → 83) + 0.26(76 → 81)	4.41	281	0.003	S_{14} (E′)	0.65(74 → 78) + 0.22(77 → 79)	4.58	271	0.055
S_{15} (E′)	−0.11(65 → 82) − 0.15(65 → 83) + 0.11(66 → 81) + 0.13(68 → 78) + 0.37(71 → 81) + 0.26(75 → 81) + 0.26(76 → 82) + 0.36(76 → 83)	4.41	281	0.003	S_{15} (E′)	0.65(73 → 78) + 0.22(77 → 80)	4.58	271	0.055
S_{17} (E′)	−0.13(63 → 78) − 0.14(74 → 78) + 0.62(77 → 79)	4.60	269	0.248	S_{17} (E′)	−0.11(63 → 78) − 0.22(74 → 78) + 0.61(77 → 79)	4.74	261	0.318
S_{18} (E′)	0.13(64 → 78) − 0.13(73 → 78) + 0.62(77 → 80)	4.60	269	0.248	S_{18} (E′)	0.11(64 → 78) − 0.22(73 → 78) + 0.61(77 → 80)	4.74	261	0.318
S_{19} (E′)	0.68(69 → 78)	4.63	268	0.005	S_{19} (E′)	0.11(67 → 79) + 0.68(68 → 78)	4.86	255	0.004
S_{20} (E′)	0.68(68 → 78)	4.63	268	0.005	S_{20} (E′)	0.11(67 → 80) + 0.68(69 → 78)	4.86	255	0.004
S_{24} (A_2'')	0.10(75 → 79) − 0.10(76 → 80) + 0.68(77 → 83)	4.76	260	0.001	S_{22}(A2″)	−0.25(65 → 79) − 0.24(66 → 80) + 0.24(71 → 78) − 0.39(75 → 80) + 0.39(76 → 79)	4.99	248	0.004
Triplet excited state									
T_1 (A_2')	0.72(77 → 78)	2.81	441	0.000	T_1 (E″)	0.54(67 → 81) − 0.39(68 → 81) + 0.39(69 → 82) + 0.54(69 → 83) − 0.14(77 → 81)	2.82	440	0.000
T_2 (E″)	0.51(67 → 81) + 0.37(68 → 82) + 0.52(68 → 83) − 0.37(69 → 81)	3.00	413	0.000	T_2 (E″)	−0.54(67 → 82) − 0.38(68 → 82) + 0.54(68 → 83) − 0.39(69 → 81))	2.82	440	0.000
T_3 (E″)	−0.51(67 → 82) − 0.38(68 → 81) − 0.36(69 → 82) + 0.52(69 → 83) + 0.15(77 → 82)	3.00	413	0.000	T_3 (A2″)	−0.53(67 → 83) + 0.55(68 → 82) − 0.54(69 → 81) + 0.14(77 → 83)	2.82	440	0.000
T_4 (A2″)	−0.50(67 → 83) − 0.52(68 → 81) + 0.53(69 → 82) + 0.15(77 → 83)	3.00	413	0.000	T_4 (A_2')	0.72(77 → 78)	2.88	430	0.000
T_5 (E′)	0.75(77 → 80)	3.42	362	0.000	T_5 (E′)	0.76(77 → 80)	3.46	359	0.000

Table 6 Selected calculated excitation energies (E), wavelengths (λ), oscillator strengths (f), and dominant excitation character for singlet (S_n) and triplet (T_n) states of the triethynyl-tri-*s*-triazine in the gas phase

B3LYP					PBE0			
Excited state Singlet excited state	Main configuration	E/eV	λ/nm	f	Excited state	Main configuration	E/eV	λ/nm	f
S_6 (E′)	−0.33(57 → 63) + 0.58(62 → 65)	4.12	301	0.013	S_6 (E′)	−0.20(58 → 63) + 0.63(62 → 64)	4.26	291	0.066
S_7 (E′)	−0.33(58 → 63) + 0.58(62 → 64)	4.12	301	0.013	S_7 (E′)	−0.20(57 → 63) + 0.63(62 → 65)	4.26	291	0.066
S_{10} (E′)	0.59(58 → 63) + 0.29(62 → 64)	4.30	289	0.529	S_{10} (E′)	0.65(58 → 63) + 0.17(62 → 64)	4.47	277	0.554
S_{11} (E′)	0.59(57 → 63) + 0.29(62 → 65)	4.30	289	0.529	S_{11} (E′)	0.65(57 → 63) + 0.17(62 → 65)	4.47	277	0.554
S_{17} (A_1'')	0.10(50 → 63) + 0.48(59 → 64) + 0.48(60 → 65)	4.45	278	0.003	S_{14} (A_1'')	−0.11(50 → 63) − 0.11(53 → 64) + 0.11(54 → 65) + 0.47(59 → 64) − 0.47(60 → 65)	4.61	269	0.003
S_{22} (E′)	−0.48(57 → 65) + 0.48(58 → 64)	5.14	241	0.202	S_{20} (E′)	0.35(56 → 65) + 0.40(57 → 64) + 0.41(58 → 65)	5.35	232	0.339
S_{23} (E′)	0.48(57 → 64) + 0.48(58 → 65)	5.14	241	0.202	S_{21} (E′)	0.35(56 → 64) + 0.40(57 → 65) − 0.40(58 → 64)	5.35	232	0.339
S_{25} (E′)	0.68(56 → 65)	5.20	239	0.210	S_{25} (E′)	0.58(56 → 65) − 0.26(57 → 64) − 0.26(58 → 65)	5.41	229	0.021
S_{26} (E′)	0.68(56 → 64)	5.20	239	0.210	S_{26} (E′)	0.58(56 → 64) − 0.26(57 → 65) + 0.26(55 → 63)	5.41	229	0.021
Triplet excited state									
T_1 (A_2')	0.72(62 → 63)		2.44 509	0.000	T_1 (A_2')	0.73(62 → 63)		2.50 496	0.000
T_2 (E′)	0.75(62 → 64)		3.08 403	0.000	T_2 (E′)	0.76(62 → 65)		3.11 398	0.000
T_3 (E′)	0.75(62 → 65)		3.08 403	0.000	T_3 (E′)	0.76(62 → 64)		3.11 398	0.000
T_4 (A_1'')	−0.16(59 → 65) − 0.16(60 → 64) + 0.67(61 → 63)		3.26 380	0.000	T_4 (A_1'')	0.59(56 → 63) − 0.33(57 → 64) − 0.14(57 → 68) + 0.33(58 → 65) − 0.14(58 → 67)		3.36 369	0.000
T_5 (E″)	0.67(59 → 63) − 0.18(61 → 65)		3.31 375	0.000	T_5 (A_1'')	0.19(59 → 65) − 0.19(60 → 64) + 0.66(61 → 63)		3.39 366	0.000

triplet excited states are all zero. Spin–orbit coupling can mix singlet character into a triplet state and thus allows the latter to acquire intensity in both absorption and emission.

3.2. Absorption in solution

We used the continuous medium theory to perform calculations for the solvent effect. Transition energies of the excited states of *s*-triazine and tri-*s*-triazines in ethanol were computed with the PCM solvation model linked to TDDFT (B3LYP and PBE0), with the aug-cc-pVDZ basis sets. The overall solvation effect on geometry is negligible. Thirty singlet and triplet-excited states were calculated at the optimized structure of the ground state in solution for each species. The corresponding UV/Vis spectra (grey curves) are displayed in Fig. 2. Again, we will use the B3LYP results in our discussion. Gillan *et al.* have recorded the absorption spectrum of triazido-tri-*s*-triazine in ethanol.[19] There are two peaks at 275 and 295 nm in their spectrum, which are in reasonable agreement with our calculated absorption peaks located at 242 and 276 nm.

In going from the gas phase to ethanol solution, a small variation for all the energy bands can be observed, while all oscillator strengths are increased. By considering the excited energy with strongest oscillator strength for each species in this study, the solvent effects produce a red shift of 0.17 eV for *s*-triazine, a blue shift of 0.01 eV for tri-*s*-triazine, a red shift of 0.09 eV for trifluoride-tri-*s*-triazine, a red shift of 0.24 eV for triamino-tri-*s*-triazine, a blue shift of 0.08 eV for trinitro-tri-*s*-triazine, a blue shift of 0.02 eV for triethynyl-tri-*s*-triazine, and a red shift of 0.04 eV for triazido-tri-*s*-triazine. As in the gas phase, most of the excited states in solution have mixed character. The dominant configurations of the excited states with strongest oscillator strengths of tri-*s*-triazines in solution are almost invariably the same as those in the gas phase. The only exception is in triamino-tri-*s*-triazine, where in solution the dominant excitation with the highest oscillator strength is 53 → 59 (π → π*); in the gas phase the most intense transition is from 50 → 59 (n → π*).

4. Conclusions

We have investigated the vertical electronic excitations of tri-*s*-triazines by using the TDDFT method. The solvation effects have been taken into account through the PCM model. Thirty singlet and triplet excited states have been examined for each species in the gas phase and in solution. Our calculations show that excitation energies calculated using PBE0 are slightly higher than those calculated using B3LYP, but the energies obtained by these two functionals are in similar order. Our computational results are in good agreement with the available experimental data. Only the excited states with highest oscillator strength in tri-*s*-triazine and triethynyl-tri-*s*-triazine give π → π* excitation and have transition energies higher than those of other tri-*s*-triazines. The energies of all bands in solution are very close to those in the gas phase, despite the oscillator strengths are higher in the solution phase.

Table 7 Selected calculated excitation energies (E), wavelengths (λ), oscillator strengths (f), and dominant excitation character for singlet (S_n) and triplet (T_n) states of the triazido-tri-*s*-triazine in the gas phase

B3LYP					PBE0				
Excited state	Main configuration	E/eV	λ/nm	f	Excited state	Main configuration	E/eV	λ/nm	f
Singlet excited state									
S_5 (E′)	−0.37(72 → 75) − 0.11(73 → 75) + 0.47(74 → 76) − 0.30(74 → 77)	4.36	284	0.015	S_5 (E′)	0.31(73 → 75) + 0.25(74 → 76) + 0.54(74 → 77)	4.55	273	0.037
S_6 (E′)	−0.11(72 → 75) + 0.37(73 → 75) + 0.30(74 → 76) + 0.47(74 → 77)	4.36	284	0.015	S_6 (E′)	−0.31(72 → 75) + 0.54(74 → 76) − 0.25(74 → 77)	4.55	273	0.037
S_7 (E′)	0.46(72 → 75) − 0.31(73 → 75) + 0.33(74 → 76) + 0.13(74 → 77)	4.53	274	0.508	S_7 (E′)	0.59(72 → 75) + 0.29(74 → 76)	4.70	264	0.603
S_8 (E′)	0.31(72 → 75) + 0.46(73 → 75) + 0.13(74 → 76) − 0.33(74 → 77)	4.53	274	0.508	S_8 (E′)	0.59(73 → 75) − 0.29(74 → 77)	4.70	264	0.603
S_{12} (A″)	−0.33(68 → 78) − 0.35(72 → 79) − 0.23(72 → 80) − 0.23(73 → 79) + 0.35(73 → 80) − 0.13(74 → 78)	4.71	263	0.001	S_{11} (A″)	0.35(68 → 78) + 0.29(72 → 79) − 0.29(72 → 80) + 0.29(73 → 79) + 0.29(73 → 80)	4.81	258	0.001
S_{18} (A″)	−0.21(69 → 76) + 0.43(69 → 77) − 0.43(70 → 76) − 0.21(70 → 77)	4.85	256	0.005	S_{15} (A″)	0.18(69 → 76) − 0.43(69 → 77) + 0.43(70 → 76) + 0.18(70 → 77)	5.01	247	0.006
S_{23} (E′)	+ 0.21(72 → 76) + 0.40(72 → 77) − 0.40(73 → 76) + 0.21(73 → 77)	5.14	241	0.254	S_{23} (E′)	−0.25(68 → 76) –0.16(72 → 76) − 0.39(72 → 77) + 0.39(73 → 76)	5.34	232	0.289
S_{24} (E′)	+ 0.40(72 → 76) − 0.21(72 → 77) + 0.21(73 → 76) + 0.40(73 → 77)	5.14	241	0.254	S_{24} (E′)	+ 0.25(68 → 77) + 0.39(72 → 76) + 0.16(73 → 76) + 0.39(73 → 77)	5.34	232	0.289
S_{26} (E′)	0.30(68 → 76) + 0.57(68 → 77)	5.27	235	0.217	S_{26} (E′)	0.38(68 → 76) + 0.47(68 → 77)	5.47	227	0.130
S_{27} (E′)	0.57(68 → 76) − 0.30(68 → 77) − 0.12(72 → 77) + 0.12(73 → 76)	5.27	235	0.217	S_{27} (E′)	0.47(68 → 76) − 0.38(68 → 77) − 0.21(72 → 77) + 0.21(73 → 76)	5.47	227	0.130
S_{28} (E′)	0.28(69 → 78) + 0.20(69 → 80) + 0.25(70 → 78) + 0.20(70 → 79) + 0.25(71 → 79) + 0.39(71 → 80)	5.43	228	0.038	S_{29} (E′)	−0.22(69 → 78) − 0.22(69 → 79) − 0.33(70 → 78) − 0.14(70 → 79) − 0.22(70 → 80) + 0.44(71 → 80)	5.74	216	0.016
S_{29} (E′)	0.25(69 → 78) − 0.28(70 → 78) + 0.39(71 → 79) − 0.25(71 → 80)	5.43	228	0.038	S_{30} (E′)	0.33(69 → 78) + 0.22(70 → 78) + 0.22(70 → 79) + 0.44(71 → 79)	5.74	216	0.016
Triplet excited state									
T_1 (A′)	0.71(74 → 75)	3.03	409	0.000	T_1 (A′)	0.71(74 → 75)	3.14	395	0.000
T_2 (E′)	0.67(74 → 76) + 0.28(74 → 77)	3.47	357	0.000	T_2 (E′)	0.22(74 → 76) + 0.69(74 → 77)	3.54	350	0.000
T_3 (E′)	− 0.28(74 → 76) + 0.67(74 → 77) − 0.10(74 → 82)	3.47	357	0.000	T_3 (E′)	0.12(72 → 75) + 0.69(74 → 76) − 0.22(74 → 77) + 0.15(74 → 82)	3.54	350	0.000
T_4 (E′)	0.23(68 → 77) + 0.18(72 → 76) + 0.60(73 → 75) + 0.18(73 → 77)	3.69	336	0.000	T_4 (A′)	0.54(68 → 75) –0.30(72 → 76) − 0.15(72 → 77) + 0.30(73 → 77)	3.73	332	0.000
T_5 (E′)	−0.23(68 → 76) + 0.60(72 → 75) − 0.18(72 → 77) + 0.18(73 → 76)	3.69	336	0.000	T_5 (E′)	0.26(68 → 77) –0.27(72 → 75) + 0.51(73 → 75) + 0.19(73 → 77)	3.74	332	0.000

Acknowledgements

This work was supported by the Research Grants Council of Hong Kong (Account no. 9040979 (CityU 102404)), the National Science Foundation of China (Account no. 20373045) and Special Research Foundation of Doctoral Education of Chinese University (Account no. 20020610024).

References

1 A. Y. Liu and M. L. Cohen, *Science*, 1989, **245**, 841.
2 D. M. Teter and R. J. Hemley, *Science*, 1996, **271**, 53.
3 T. Malkow, *Mater. Sci. Eng., A*, 2001, **302**, 311.
4 S. Matsumoto, E. Q. Xie and F. Izumi, *Diamond Relat. Mater.*, 1999, **8**, 1175.
5 S. Matsumoto, E. Q. Xie and F. Izumi, *Diamond Relat. Mater.*, 2000, **9**, 94.
6 L. R. Shaginyan, *Powder Metal. Met. Ceram.*, 1999, **37**, 648.
7 P. F. McMillan, *Curr. Opin. Solid State Mater. Sci.*, 1999, **4**, 171.
8 V. J. Badding, *Adv. Mater.*, 1997, **9**, 877.
9 E. Kroke, M. Schwarz, E. Horath-Bordon, P. Kroll, B. Noll and A. D. Norman, *New J. Chem.*, 2002, **26**, 508.
10 J. Liebig, *Ann. Pharm.*, 1834, **10**, 10.
11 L. Gmelin, *Ann. Pharm.*, 1835, **15**, 252.
12 L. Pauling and J. H. Sturdivant, *Proc. Natl. Acad. Sci. USA*, 1937, **23**, 615.
13 E. K. Wilson, *Chem. Eng. News*, 2000, **78**(32), 62.
14 M. A. Rossman, N. J. Leonard, S. Urano and P. R. LeBreton, *J. Am. Chem. Soc.*, 1985, **107**, 3884.
15 R. S. Hosmane, M. A. Rossman and N. J. Leonard, *J. Am. Chem. Soc.*, 1982, **104**, 5497.
16 M. Shahbaz, S. Urano, P. R. LeBreton, M. A. Rossman, R. S. Hosmane and N. J. Leonard, *J. Am. Chem. Soc.*, 1984, **106**, 2805.
17 B. Jürgens, E. Irran, J. Senker, P. Kroll, H. Müller and W. Schnick, *J. Am. Chem. Soc.*, 2003, **125**, 10288.
18 D. R. Miller, D. C. Swenson and E. G. Gillan, *J. Am. Chem. Soc.*, 2004, **126**, 5372.
19 (*a*) C. E. Redemann and H. J. Lucas, *J. Am. Chem. Soc.*, 1940, **62**, 842–1; (*b*) H. Schroeder and E. Kober, *J. Org. Chem.*, 1962, **27**, 4262–1; (*c*) H. Schroeder (Olin Mathieson Chem. Corp. Virginia, USA), US Pat. 3089875, 1963; (*d*) A. I. Finkelshtein and N. V. Spiridonova, *Russ. Chem. Rev.*, 1964, **33**, 400; (*e*) R. Neef (Bayer AG Leverkusen, Germany), Ger. Pat., DE1102321, 1961; (*f*) C. Gremmelmaier and J. Riethmann (Ciba-Geigy, New York, USA), US Pat., US 4205167 A, 1980.
20 W. X. Zheng, N.-B. Wong, W. Z. Wang, G. Zhou and A. M. Tian, *J. Phys. Chem. A*, 2004, **108**, 97.
21 W. X. Zheng, N.-B. Wong, X. Q. Liang, X. P. Long and A. M. Tian, *J. Phys. Chem. A*, 2004, **108**, 840.
22 W. X. Zheng, N.-B. Wong, G. Zhou, X. Q. Liang, J. S. Li and A. M. Tian, *New J. Chem.*, 2004, **28**, 275.
23 W. X. Zheng, N.-B. Wong, W.-K. Li and A. M. Tian, *J. Phys. Chem. A*, 2004, **108**, 11721.
24 S. Hirata, S. Ivanov, I. Grabowski and R. J. Bartlett, *J. Chem. Phys.*, 2002, **116**, 6468.
25 R. Bauernschmitt and R. Ahlrichs, *Chem. Phys. Lett.*, 1996, **256**, 454.
26 N. C. Handy and D. J. Tozer, *J. Comput. Chem.*, 1999, **20**, 106.
27 A. S. Zyubin and A. M. Mebel, *J. Chem. Phys.*, 2003, **119**, 6581.
28 C. Adamo and V. Barone, *Chem. Phys. Lett.*, 2000, **330**, 152.
29 C. J. Jödicke and H. P. Lüthi, *J. Chem. Phys.*, 2002, **117**, 4146.
30 C. J. Jödicke and H. P. Lüthi, *J. Am. Chem. Soc.*, 2003, **125**, 252.
31 C. Neiss, P. Saalfrank, M. Parac and S. Grimme, *J. Phys. Chem. A*, 2003, **107**, 140.
32 M. K. Casida, C. Jamorski, K. C. Casida and D. R. Salahub, *J. Chem. Phys.*, 1998, **108**, 4439.
33 J. Tozer and N. C. Handy, *J. Chem. Phys.*, 1998, **109**, 10180.
34 C. Adamo and V Barone, *J. Chem. Phys.*, 1999, **110**, 6158.
35 J. P. Perdew, K. Burke and M. Ernzerhof, *Phys. Rev. Lett.*, 1996, **77**, 3865.
36 C. Adamo, G. E. Scuseria and V. Barone, *J. Chem. Phys.*, 1999, **111**, 2889.
37 C. Adamo and V. Barone, *Chem. Phys. Lett.*, 1999, **314**, 152.
38 B. Mennucci, R. Cammi and J Tomasi, *J. Chem. Phys.*, 1998, **109**, 2798.
39 M. Cossi and V. Barone, *J. Chem. Phys.*, 2001, **115**, 4708.
40 M. J. Frisch, G. W. Trucks, H. B. Schlegel, G. E. Scuseria, M. A. Robb, J. R. Cheeseman, J. A. Montgomery Jr, T. Vreven, K. N. Kudin, J. C. Burant, J. M. Millam, S. S. Iyengar, J. Tomasi, V. Barone, B. Mennucci, M. Cossi, G. Scalmani, N. Rega, G. A. Petersson, H. Nakatsuji, M. Hada, M. Ehara, K. Toyota, R. Fukuda, J. Hasegawa, M. Ishida, T. Nakajima, Y. Honda, O. Kitao, H. Nakai, M. Klene, X. Li, J. E. Knox, H. P. Hratchian, J. B. Cross, C. Adamo, J. Jaramillo, R. Gomperts, R. E. Stratmann, O. Yazyev, A. J. Austin, R. Cammi, C. Pomelli, J. W. Ochterski, P. Y. Ayala, K. Morokuma, G. A. Voth, P. Salvador, J. J. Dannenberg, V. G. Zakrzewski, S. Dapprich, A. D. Daniels, M. C. Strain, O. Farkas, D. K. Malick, A. D. Rabuck, K. Raghavachari, J. B. Foresman, J. V. Ortiz, Q. Cui, A. G. Baboul, S. Clifford, J. Cioslowski, B. B. Stefanov, G. Liu, A. Liashenko, P. Piskorz, I. Komaromi, R. L. Martin, D. J. Fox, T. Keith, M. A. Al-Laham, C. Y. Peng, A. Nanayakkara, M. Challacombe, P. M. W. Gill, B. Johnson, W. Chen, M. W. Wong, C. Gonzalez and J. A. Pople, *GAUSSIAN 03 (Revision B05)*, Gaussian, Inc., Pittsburgh PA, 2003.
41 A. D. Becke, *J. Chem. Phys.*, 1996, **104**, 1040.
42 J. P. Perdew, M. Ernzerhof and K. Burke, *J. Chem. Phys.*, 1996, **105**, 9982.
43 A. D. Becke, *J. Chem. Phys.*, 1993, **98**, 5648.
44 C. Lee, W. Yang and R. G. Parr, *Phys. Rev. B*, 1988, **37**, 785.
45 D. E. Woon and T. H. Dunning, *J. Chem. Phys.*, 1993, **98**, 1358.
46 S. Miertus, E. Scrocco and J. Tomasi, *Chem. Phys.*, 1981, **55**, 117.
47 V. Barone, M. Cossi and J. Tomasi, *J. Chem. Phys.*, 1997, **107**, 3210.
48 D. M. Chipman, *J. Chem. Phys.*, 2000, **112**, 5558.
49 M. Cossi, N. Rega, G. Scalmani and V. Barone, *J. Chem. Phys.*, 2001, **114**, 5691.
50 A. Bolovinos, P. Tsekeris, J. Philis, E. Pantos and G. Andritsopoulus, *J. Mol. Spectrosc.*, 1984, **103**, 240.

